ResearchGate

See discussions, stats, and author profiles for this publication at: https://www.researchgate.net/publication/236218394

Rational Development of Ternary Alloy Electrocatalysts

ARTICLE *in* JOURNAL OF PHYSICAL CHEMISTRY LETTERS · JUNE 2012

Impact Factor: 7.46 · DOI: 10.1021/jz300563z

CITATIONS
42

READS
41

12 AUTHORS, INCLUDING:

Dongguo Li
Brown University
19 PUBLICATIONS **909** CITATIONS
SEE PROFILE

Miaofang Chi
Oak Ridge National Laboratory
149 PUBLICATIONS **4,679** CITATIONS
SEE PROFILE

John E Pearson
Argonne National Laboratory
226 PUBLICATIONS **5,224** CITATIONS
SEE PROFILE

Zhiyao Duan
University of Pittsburgh
12 PUBLICATIONS **138** CITATIONS
SEE PROFILE

Available from: Dennis van der Vliet
Retrieved on: 29 January 2016

THE JOURNAL OF PHYSICAL CHEMISTRY Letters

Letter

pubs.acs.org/JPCL

Rational Development of Ternary Alloy Electrocatalysts

Chao Wang,[†] Dongguo Li,[†,‡] Miaofang Chi,[§] John Pearson,[†] Rees B. Rankin,[⊥] Jeff Greeley,[⊥] Zhiyao Duan,[#] Guofeng Wang,[#] Dennis van der Vliet,[†] Karren L. More,[§] Nenad M. Markovic,[†] and Vojislav R. Stamenkovic*[,†]

[†]Materials Science Division and [⊥]Center for Nanoscale Materials, Argonne National Laboratory, Argonne, Illinois 60439, United States

[‡]Department of Chemistry, Brown University, Providence, Rhode Island 02912, United States

[§]Division of Material Science and Technology, Oak Ridge National Laboratory, Oak Ridge, Tennessee 37831, United States

[#]Department of Mechanical Engineering & Materials Science, University of Pittsburgh, Pennsylvania, Pennsylvania 15260, United States

Supporting Information

ABSTRACT: Improving the efficiency of electrocatalytic reduction of oxygen represents one of the main challenges for the development of renewable energy technologies. Here, we report the systematic evaluation of Pt-ternary alloys ($Pt_3(MN)_1$ with M, N = Fe, Co, or Ni) as electrocatalysts for the oxygen reduction reaction (ORR). We first studied the ternary systems on extended surfaces of polycrystalline thin films to establish the trend of electrocatalytic activities and then applied this knowledge to synthesize ternary alloy nanocatalysts by a solvothermal approach. This study demonstrates that the ternary alloy catalysts can be compelling systems for further advancement of ORR electrocatalysis, reaching higher catalytic activities than bimetallic Pt alloys and improvement factors of up to 4 versus monometallic Pt.

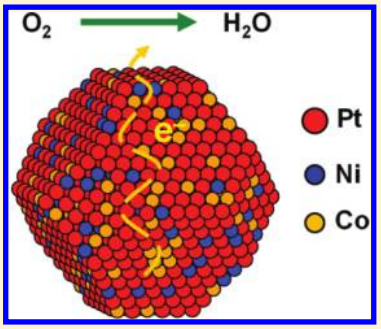

SECTION: Surfaces, Interfaces, Porous Materials, and Catalysis

Highly efficient catalysts for the oxygen reduction reaction (ORR) have been studied for the development of renewable energy technologies such as fuel cells[1] and metal–air batteries.[2,3] The current state-of-the-art electrocatalyst for this reaction is Pt in the form of nanoparticles (NPs) supported on high-surface-area carbon. Even though Pt is considered to be the catalyst of choice, the kinetic limitation for the ORR is substantial, resulting in loss of potential at which this reaction is taking place. In addition, the high cost and scant availability of Pt have further limited commercial applications of technologies that rely on precious metal catalysts with high rates for the ORR. Hence, one of the major efforts in the development of renewable energy technologies is to improve the performance of ORR catalysts and reduce the amount of Pt needed.

Alloying has been shown to be a promising approach to producing advanced catalytic materials.[4−10] Previous work on extended surfaces (bulk electrodes) has demonstrated that bimetallic Pt_3M (M = Fe, Co, Ni, etc.) alloys are superior for the ORR when compared to Pt, with the enhanced catalytic activity arising from the altered electronic structures of the topmost Pt atoms.[8,11,12] This modification has been found to reduce the surface coverage by oxygenated spectator species (e.g., OH^-) and thus increase the number of active sites accessible for molecular oxygen.[8,12]

So far, the focus has been largely placed on Pt-bimetallic catalysts, but other systems, such as ternary alloys, have also attracted substantial interest due to the potential for fine-tuning of the electronic structures and further improving the catalytic activity.[13−26] Though high-surface-area nanocatalysts have been intensively studied,[19−22] extended surfaces of Pt-ternary alloys have not been thoroughly investigated for the ORR,[23−26] and the trend of catalytic activity for the Pt-ternary catalysts has not been established yet. Moreover, the correlation between electronic structures and surface adsorption/catalytic properties still remains elusive for such multimetallic systems, which however is important for fundamental understanding of the enhanced catalysis and achieving rational catalyst design. Therefore, more systematic studies are needed for full exploration of Pt-based multimetallic systems in electrocatalysis.

In this Letter, we focus on $Pt_3(MN)_1$ alloy catalysts for electrocatalytic reduction of oxygen. The main objective of this study is to perform systematic evaluation of Pt-ternary alloys versus Pt-bimetallic systems. For that purpose, we first investigate well-defined extended surfaces of ternary thin-film alloys to examine their electrocatalytic activities and then develop a NP synthesis for the ternary system of choice. In addition, we also performed theoretical simulations based on density functional theory (DFT) and have been able to extend

Received: May 3, 2012
Accepted: June 1, 2012
Published: June 1, 2012

 © 2012 American Chemical Society dx.doi.org/10.1021/jz300563z | J. Phys. Chem. Lett. 2012, 3, 1668–1673

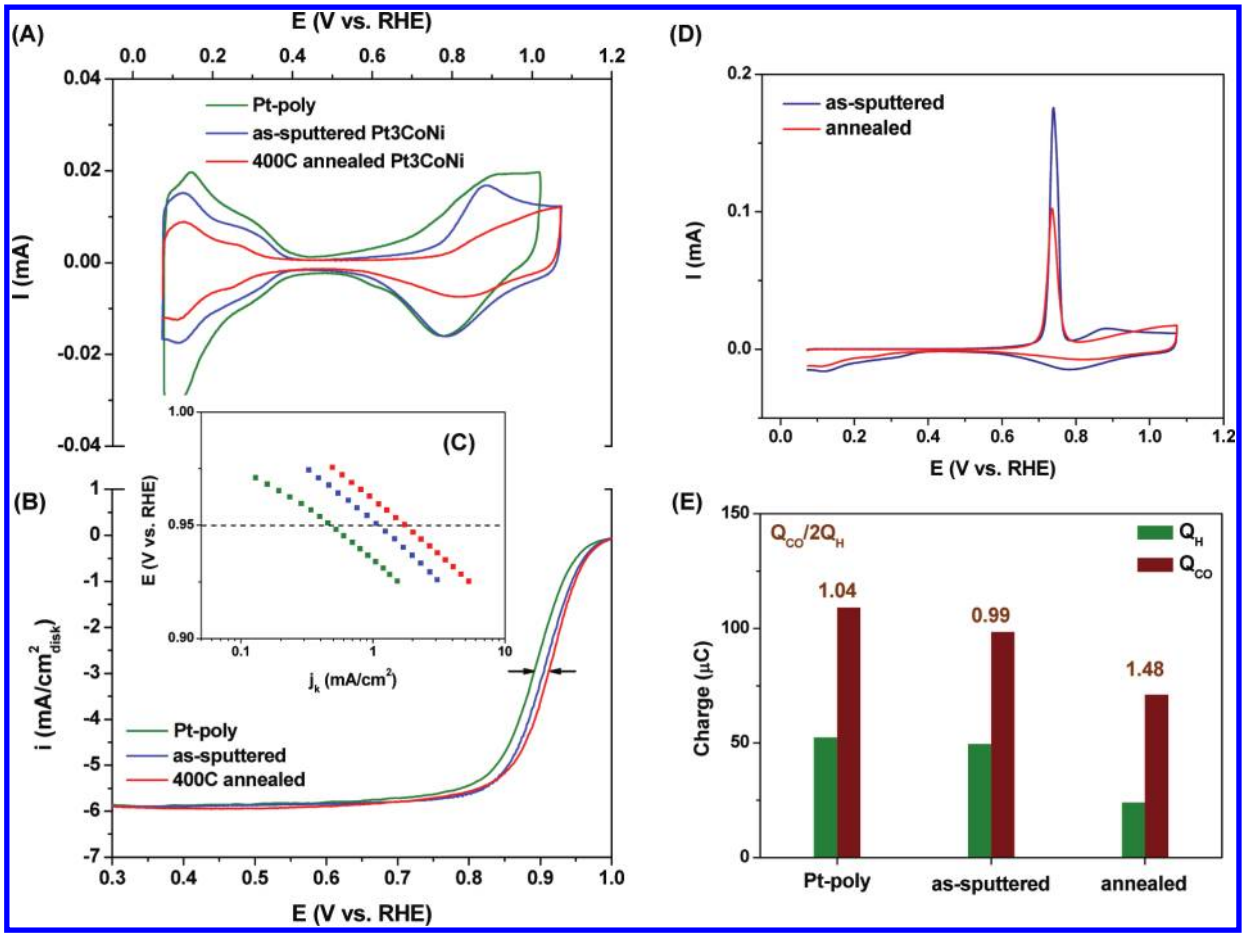

Figure 1. Electrochemical characterization of the extended $Pt_3(CoNi)_1$ thin-film surfaces. (A) Cyclic voltammograms (CVs), (B) polarization curves, and (C) Tafel plots. Specific activities for the ternary systems were presented as kinetic currents normalized by ECSAs obtained from CO_{ad} stripping curves. (D) CO stripping curves of the as-sputtered and annealed $Pt_3(CoNi)_1$ surfaces. (E) H_{upd} (Q_H) and CO stripping (Q_{CO}) integrated charges from (A) and (D), with the ratio of $Q_{CO}/2Q_H$ labeled above the histogram bars.

previously established relationships between electronic structures and catalytic performance from Pt-bimetallic to Pt-ternary systems.

Polycrystalline ternary films of 50 nm in thickness were prepared by confocal magnetron sputtering. Different targets of pure metals were used for sputtering over a mirror polished glassy carbon substrate of 6 mm in diameter. The obtained films were subjected to annealing to induce a homogeneous elemental distribution and subsequent surface analyses in order to explore the existence of Pt-skin formation in ternary systems (see the Methods in the Supporting Information (SI)).[27,28] Figure 1 summarizes the results of electrochemical studies for these thin films acquired by a rotating disk electrode (RDE). Compared to polycrystalline Pt (Pt-poly), cyclic voltammograms (CVs, Figure 1A) of the as-sputtered films have similar features in the underpotentially deposited hydrogen (H_{upd}) region ($E < 0.4$ V) with slightly suppressed peaks. In the ORR-relevant region ($E > 0.6$ V), the ternary alloy surfaces exhibit positive shifts for the onset of $Pt-OH_{ad}$ formation compared to Pt-poly, indicating weaker chemisorptions of oxygenated species on these surfaces. After annealing at 400 °C, the H_{upd} peaks of ternary systems are additionally suppressed, while the onset of $Pt-OH_{ad}$ formation is shifted to even more positive potentials. Even though both effects can also be assigned to altered surface morphology upon thermal annealing, in what follows we prove that they are predominantly associated with the formation of a Pt-skin structure due to Pt segregation.[8,28]

The surfaces of the annealed ternary thin films were examined by electrooxidation of adsorbed CO molecules. Figure 1D shows the CO stripping curves for the two types of $Pt_3(CoNi)_1$ surfaces, as sputtered and annealed. Both curves have a sharp peak at ~0.74 V, but the annealed surface exhibits lower peak intensity than the as-sputtered surface due to smoother morphology. The integrated charge of the CO stripping curves that are associated with electrooxidation of adsorbed CO are summarized in Figure 1E. The as-sputtered $Pt_3(CoNi)_1$ surface has a CO stripping charge of 98.4 μC, which is close to the value obtained for Pt-poly (109 μC) of the same geometric size (d = 6 mm). The charge of CO stripping for the annealed surface is 71.0 μC, which is about 30% lower than that of the as-sputtered surface and polycrystalline Pt. However, integration of the corresponding H_{upd} region revealed that the annealed ternary thin film exhibits suppression of H_{upd} of about ~50% after annealing (from 49.6 to 24.0 μC), as depicted in Figure 1E. Consequently, the calculated ratio $Q_{CO}/2Q_H$ increased from 0.99 to 1.48 upon annealing. This behavior is typical for the Pt-skin surface formation due to the unique electrochemical adsorption properties associated with these surfaces (Figure S1, SI). As shown in our recent studies, the ratio between CO stripping and H_{upd} charges, $Q_{CO}/2Q_H$, is a good descriptor of the surface compositional profile in the case

dx.doi.org/10.1021/jz300563z | J. Phys. Chem. Lett. 2012, 3, 1668−1673

of Pt alloys, with the value close to 1 for Pt and Pt-skeleton surfaces, and higher values revealing the formation of a Pt-skin surface due to the suppressed surface coverage by H_{upd}.[29]

The formed Pt-skin surface is expected to possess enhanced ORR catalytic activity, which was validated by polarization curves recorded by rotating disk electrode (RDE) measurements (Figure 1B). Compared to the Pt-poly surface, the as-sputtered and annealed $Pt_3(CoNi)_1$ surfaces show positive shifts of half-wave potentials, 12 and 22 mV, respectively. The specific activity at 0.95 V of the annealed surface reaches 1.75 mA/cm^2, whereas the as-sputtered surface achieves 1.12 mA/cm^2 (Figure 1C). These values correspond to improvement factors of 4 and 2.5 compared to Pt-poly (0.45 mA/cm^2), respectively.

The same strategy was employed to investigate other binary and ternary systems, and hence, a trend in the ORR activity has been established. Figure 2A shows a summary of the ORR catalytic activities of the ternaries in comparison to Pt-poly and Pt_3Co. All of the as-sputtered thin-film surfaces show higher activities than Pt-poly, with the improvement factors ranging from 1.7 to 2.5. Further improvement was consistently achieved by thermal annealing, which confirms Pt-skin surface formation for each ternary system. For the annealed surfaces, $Pt_3(CoNi)_1$ shows an improvement factor of ~4 versus Pt-poly, compared to ~2.2 and ~3.0 for $Pt_3(FeCo)_1$ and $Pt_3(FeNi)_1$, respectively.

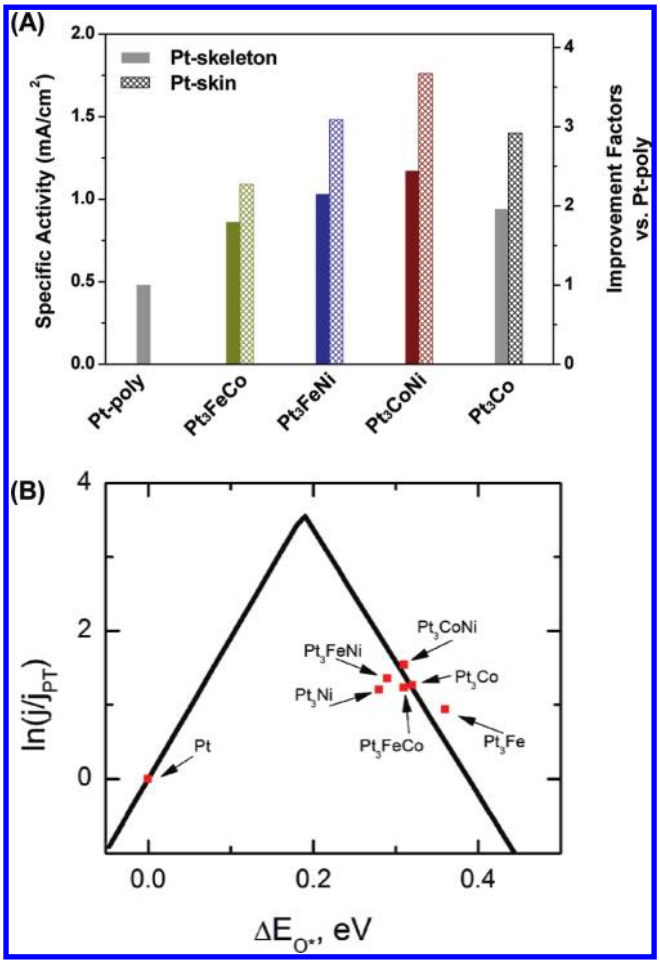

Figure 2. (A) Summary of the ORR catalytic activities for the Pt-bimetallic and Pt-ternary thin films compared to that of Pt-poly. Activities of as-sputtered (Pt-skeleton) and annealed (Pt-skin) surfaces are represented by solid and net-filled bars, respectively, with the improvement factors labeled by the right axis. (B) Volcano plot relationship of measured catalyst performance versus the DFT-calculated oxygen binding energy. The adsorption energy of oxygen (ΔE_{O*}) is calculated relative to Pt(111); activities are scaled by values measured for Pt. (Solid black activity lines are taken from DFT calculations used for Pt-based bimetallic catalysts.[30,31])

Figure 2B shows the relationship between the measured and predicted ORR activities based on the DFT-determined oxygen binding energies (see SI for additional details). It has been previously shown that the DFT approach can be utilized to generate volcano plots relating catalyst activity to a few key catalytic descriptors.[31−33] For the ORR, these and other related studies have shown that the binding energy of atomic oxygen, ΔE_{O*}, serves as a reliable descriptor. The volcano relationship in Figure 2B shows that, as is the case with binary Pt alloys, the ternary systems exhibit weaker oxygen binding compared to pure Pt. The weakening of the oxygen binding energy actually induces a change in the predicted rate-limiting step of the ORR ($O_2(g) + H^+ + e^- + * \rightarrow OOH*$ on the weak-binding side of the volcano, as opposed to $OH* + H^+ + e^- \rightarrow H_2O(l) + *$ on the strong-binding side), and both binaries and ternaries thus fall on the opposite side of the volcano from pure Pt. The net activity of the binaries and ternaries, however, is still higher than that of Pt, which is in good agreement with our experimental results. Though it remains unclear why $Pt_3(CoNi)_1$ is the most active based on the current simulations, it is evident that the employment of multimetallic Pt-based alloys can serve to additionally tune the oxygen binding energies of Pt-based catalysts, which in turn results from corresponding changes in the electronic structures of platinum surface sites.[30]

On the basis of the established trend on extended surfaces, we aimed toward the synthesis of the most active $Pt_3(CoNi)_1$ nanocatalysts. Considering that conventional impregnation methods rely on precipitation from the aqueous solutions and usually do not provide NPs with homogeneous compositions, we developed an organic solvothermal approach for the synthesis of ternary alloy NPs.[34,35] In general, Pt in solution tends to nucleate faster than the 3d transition metals and forms unalloyed Pt NPs due to the higher reduction potential of Pt^{2+} (+1.2 V) versus those of 3d metals (−0.2 to −0.4 V). However, we managed to achieve simultaneous growth for ternary alloy NPs by injection of the Pt precursor to a hot solution of the 3d transition-metal acetates (see the Methods in the SI), where 3d metal precursors could already be reduced to form metallic species and thus be able to match the fast reduction of Pt^{2+} to form uniform ternary alloy NPs.[36]

Figure 3A shows a representative transmission electron microscopy (TEM) image of the as-synthesized $Pt_3(CoNi)_1$ NPs. The monodisperse particles have an average particle size of ~6 nm, which is close to the optimal size for Pt alloy catalysts established before.[37] Elemental composition was analyzed by energy-dispersive X-ray spectroscopy (EDX), showing a composition of $Pt_{0.72}Co_{0.11}Ni_{0.17}$ close to the expected Pt/M/N = 3:0.5:0.5 ratio. In addition, distribution of elements in the ternary NPs was mapped by EDX based on high-angle annular dark field scanning transmission electron microscopy (HAADF-STEM). Figure 3B−E presents overlapped and separate maps of the elements in a typical $Pt_3(CoNi)_1$ particle. It is obvious that all of the constituents, Pt, Co, and Ni, are uniformly distributed across the particle and well intermixed in the overlapping map (Figure 3B). The observations here are consistent with our recent findings on Pt-

dx.doi.org/10.1021/jz300563z | J. Phys. Chem. Lett. 2012, 3, 1668−1673

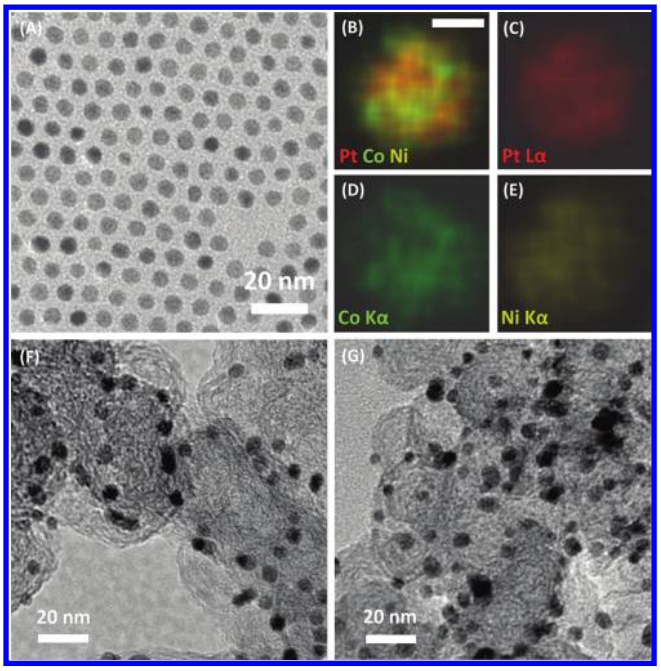

Figure 3. TEM image of the as-synthesized $Pt_3(CoNi)_1$ alloy NPs. (B–E) Representative elemental maps from EDS analysis based on STEM for (B) overlapping of Pt, Co, and Ni, (C) Pt, (D) Co, and (E) Ni. The scale bar in (B) is equal to 2 nm, and it also applies for (C–E). (F,G) TEM images of the ternary catalyst before (F) and after (G) surfactant removal and thermal treatment.

bimetallic NPs prepared by similar methods,[35] confirming the highly homogeneous nature of the ternary alloy NPs obtained by organic solution synthesis.

To prepare electrocatalysts, the as-synthesized NPs were mixed with high-surface-area carbon black (see the SI for experimental details). The previously established protocol for thermal treatment was applied to remove the surfactants and induce beneficial surface segregation for best catalytic performance.[38,39] TEM images (Figure 3F and G) show that no significant size or morphology change happened after these treatments. A catalyst suspension was prepared by sonication of the catalyst in deionized water, and a drop of that suspension was deposited on a polished glassy carbon (GC) disk (6 mm in diameter). The content of Pt in the catalyst was adjusted to ~25%, and the loading of Pt on the GC electrode was ~12 $\mu g/cm^2_{disk}$.

Figure 4 summarizes electrochemical results for the $Pt_3(CoNi)_1$ nanocatalysts and commercial Pt/carbon of a similar size (6 nm, Tanaka), which was used as a reference. The measured CVs have H_{upd} peaks at $E < 0.4$ V and Pt oxidation/reduction peaks at 0.8–0.9 V. Similar to the results on extended surfaces (Figure 1A), the onset of $Pt-OH_{ad}$ on the ternary catalyst was shifted positively by >25 mV versus Pt/C (Figure 4A), confirming altered electronic structures and surface adsorption properties of ternary alloy NPs. Consequently, the corresponding polarization curves exhibit similar shifts in half-wave potentials and show substantially enhanced catalytic activities (Figure 4B). At 0.95 V, the as-prepared and annealed $Pt_3(CoNi)_1/C$ catalysts have achieved improvement factors of 2.3 and 4.2 in specific activity versus Pt/C (Figure 4C), with the annealed catalyst reaching 0.55 mA/cm^2 (versus 0.13 mA/cm^2 for Pt/C). The level of catalytic activity improvement is consistent with the trend established on extended thin-film

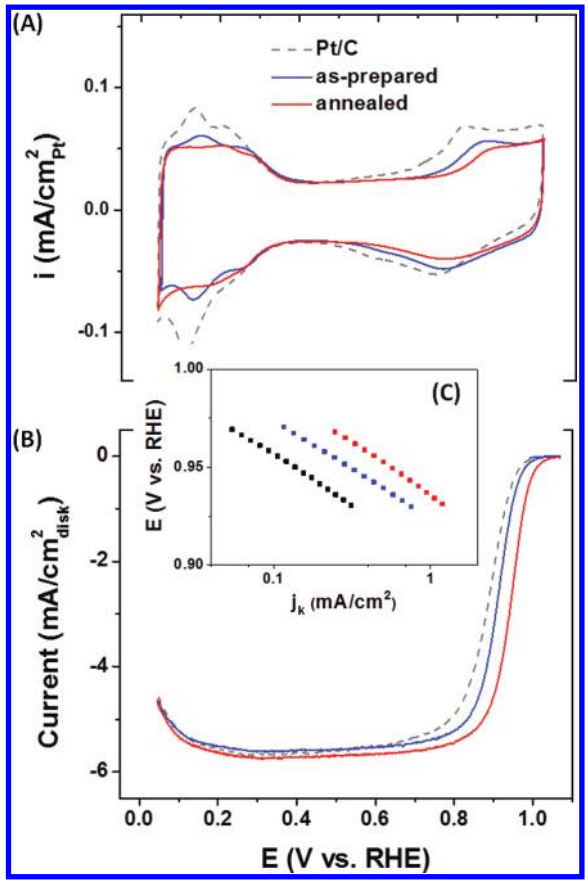

Figure 4. Electrochemical characterization of the $Pt_3(CoNi)_1/C$ catalysts. (A) CVs recorded at 50 mV/s in Ar-saturated 0.1 M $HClO_4$. (B) Polarization curves for the ORR with the *iR* drop correction recorded in O_2-saturated 0.1 M $HClO_4$. (C) Tafel plots of the kinetic current densities depending on electrode potentials.

surfaces. Similar improvement factors were also present in mass activity, with the annealed $Pt_3(CoNi)_1/C$ achieving 183 A/g in comparison to 49 A/g for Pt/C.

Ternary alloys of Pt and 3d transition metals were investigated as catalysts for the ORR. Systematic studies on extended surfaces of Pt-based ternary thin films revealed a volcano-type dependence between the measured catalytic activities and DFT-predicted oxygen-binding energies of corresponding model ternary alloy surfaces. On the basis of this trend, we have synthesized the catalyst of choice with the highest activity based on monodisperse and homogeneous ternary alloy NPs from organic solution synthesis. Our comparative studies show that the ternary alloy catalysts possess enhanced catalytic activities for the ORR when compared to Pt or Pt-bimetallic alloys. The most active system was found to be $Pt_3(CoNi)_1$, which exhibits an improvement factor of ~4 versus Pt.

■ ASSOCIATED CONTENT

Ⓢ Supporting Information

More material characterizations. This material is available free of charge via the Internet at http://pubs.acs.org.

■ AUTHOR INFORMATION

Corresponding Author

*E-mail: vrstamenkovic@anl.gov.

Notes

The authors declare no competing financial interest.

■ ACKNOWLEDGMENTS

This work was conducted at Argonne National Laboratory, a U.S. Department of Energy, Office of Science Laboratory, operated by UChicago Argonne, LLC, under Contract No. DE-AC02-06CH11357. This research was sponsored by the U.S. Department of Energy, Office of Energy Efficiency and Renewable Energy, Fuel Cell Technologies Program. Other components of the research, including a DOE Early Career Award (J.G.) and use of the Center for Nanoscale Materials, was supported by the U.S. Department of Energy, Office of Science, Office of Basic Energy Sciences. Microscopy research was conducted at the Electron Microscopy Center for Materials Research at Argonne. STEM and element mapping were done at ORNL's SHaRE User Facility sponsored by the Scientific User Facilities Division, Office of Basic Energy Sciences, the U.S. Department of Energy.

■ REFERENCES

(1) Vielstich, W.; Lamm, A.; Gasteiger, H. A. *Handbook of Fuel Cells: Fundamentals, Technology, And Applications*; Wiley: New York, 2003.
(2) Abraham, K. M.; Jiang, Z. A Polymer Electrolyte-Based Rechargeable Lithium/Oxygen Battery. *J. Electrochem. Soc.* **1996**, *143*, 1−5.
(3) Armand, M.; Tarascon, J. M. Building Better Batteries. *Nature* **2008**, *451*, 652−657.
(4) Besenbacher, F.; Chorkendorff, I.; Clausen, B. S.; Hammer, B.; Molenbroek, A. M.; Norskov, J. K.; Stensgaard, I. Design of a Surface Alloy Catalyst for Steam Reforming. *Science* **1998**, *279*, 1913−1915.
(5) Diemant, T.; Hager, T.; Hoster, H. E.; Rauscher, H.; Behm, R. J. Hydrogen Adsorption and Coadsorption with CO on Well-Defined Bimetallic PtRu Surfaces — A Model Study on the CO Tolerance of Bimetallic PtRu Anode Catalysts in Low Temperature Polymer Electrolyte Fuel Cells. *Surf. Sci.* **2003**, *541*, 137−146.
(6) Greeley, J.; Mavrikakis, M. Alloy Catalysts Designed from First Principles. *Nat. Mater.* **2004**, *3*, 810−815.
(7) Chen, M. S.; Kumar, D.; Yi, C. W.; Goodman, D. W. The Promotional Effect of Gold in Catalysis by Palladium−Gold. *Science* **2005**, *310*, 291−293.
(8) Stamenkovic, V. R.; Mun, B. S.; Arenz, M.; Mayrhofer, K. J. J.; Lucas, C. A.; Wang, G. F.; Ross, P. N.; Markovic, N. M. Trends in Electrocatalysis on Extended and Nanoscale Pt-Bimetallic Alloy Surfaces. *Nat. Mater.* **2007**, *6*, 241−247.
(9) Strasser, P.; Koh, S.; Anniyev, T.; Greeley, J.; More, K.; Yu, C. F.; Liu, Z. C.; Kaya, S.; Nordlund, D.; et al. A. Lattice-Strain Control of the Activity in Dealloyed Core−Shell Fuel Cell Catalysts. *Nature Chem.* **2010**, *2*, 454−460.
(10) Tao, F.; Grass, M. E.; Zhang, Y. W.; Butcher, D. R.; Aksoy, F.; Aloni, S.; Altoe, V.; Alayoglu, S.; et al. Evolution of Structure and Chemistry of Bimetallic Nanoparticle Catalysts under Reaction Conditions. *J. Am. Chem. Soc.* **2010**, *132*, 8697−8703.
(11) Stamenkovic, V.; Mun, B. S.; Mayrhofer, K. J. J.; Ross, P. N.; Markovic, N. M.; Rossmeisl, J.; Greeley, J.; Norskov, J. K. Changing the Activity of Electrocatalysts for Oxygen Reduction by Tuning the Surface Electronic Structure. *Angew. Chem., Int. Ed.* **2006**, *45*, 2897−2901.
(12) Stamenkovic, V. R.; Fowler, B.; Mun, B. S.; Wang, G. F.; Ross, P. N.; Lucas, C. A.; Markovic, N. M. Improved Oxygen Reduction Activity on $Pt_3Ni(111)$ via Increased Surface Site Availability. *Science* **2007**, *315*, 493−497.
(13) Seo, A.; Lee, J.; Han, K.; Kim, H. Performance and Stability of Pt-Based Ternary Alloy Catalysts for PEMFC. *Electrochim. Acta* **2006**, *52*, 1603−1611.
(14) Antolini, E. Platinum-Based Ternary Catalysts for Low Temperature Fuel Cells Part I. Preparation Methods and Structural Characteristics. *Appl. Catal., B* **2007**, *74*, 324−336.
(15) Antolini, E. Platinum-Based Ternary Catalysts for Low Temperature Fuel Cells Part II. Electrochemical Properties. *Appl. Catal., B* **2007**, *74*, 337−350.
(16) Neyerlin, K. C.; Srivastava, R.; Yu, C. F.; Strasser, P. Electrochemical Activity and Stability of Dealloyed Pt−Cu and Pt−Cu−Co Electrocatalysts for the Oxygen Reduction Reaction (ORR). *J. Power Sources* **2009**, *186*, 261−267.
(17) Srivastava, R.; Mani, P.; Hahn, N.; Strasser, P. Efficient Oxygen Reduction Fuel Cell Electrocatalysis on Voltammetrically Dealloyed Pt−Cu−Co Nanoparticles. *Angew. Chem., Int. Ed.* **2007**, *46*, 8988−8991.
(18) Mani, P.; Srivastava, R.; Strasser, P. Dealloyed Binary PtM_3 (M = Cu, Co, Ni) and Ternary $PtNi_3M$ (M = Cu, Co, Fe, Cr) Electrocatalysts for the Oxygen Reduction Reaction: Performance in Polymer Electrolyte Membrane Fuel Cells. *J. Power S.* **2011**, *196*, 666−673.
(19) Neyerlin, K. C.; Bugosh, G.; Forgie, R.; Liu, Z. C.; Strasser, P. Combinatorial Study of High-Surface-Area Binary and Ternary Electrocatalysts for the Oxygen Evolution Reaction. *J. Electrochem. Soc.* **2009**, *156*, B363−B369.
(20) Fang, B.; Luo, J.; Chen, Y. S.; Wanjala, B. N.; Loukrakpam, R.; Hong, J. A.; Yin, J.; Hu, X. A.; Hu, P. P.; Zhong, C. J. Nanoengineered PtVFe/C Cathode Electrocatalysts in PEM Fuel Cells: Catalyst Activity and Stability. *ChemCatChem* **2011**, *3*, 583−593.
(21) Datta, J.; Dutta, A.; Mukherjee, S. The Beneficial Role of the Cometals Pd and Au in the Carbon-Supported PtPdAu Catalyst Toward Promoting Ethanol Oxidation Kinetics in Alkaline Fuel Cells: Temperature Effect and Reaction Mechanism. *J. Phys. Chem. C* **2011**, *115*, 15324−15334.
(22) Wanjala, B. N.; Loukrakpam, R.; Luo, J.; Njoki, P. N.; Mott, D.; Zhong, C. J.; Shao, M. H.; Protsailo, L.; Kawamura, T. Thermal Treatment of PtNiCo Electrocatalysts: Effects of Nanoscale Strain and Structure on the Activity and Stability for the Oxygen Reduction Reaction. *J. Phys. Chem. C* **2010**, *114*, 17580−17590.
(23) Miura, A.; Tague, M. E.; Gregoire, J. M.; Wen, X. D.; van Dover, R. B.; Abruna, H. D.; DiSalvo, F. J. Synthesis of Pt−Mo−N Thin Film and Catalytic Activity for Fuel Cells. *Chem. Mater.* **2010**, *22*, 3451−3456.
(24) He, T.; Kreidler, E. Combinatorial screening of PtTiMe ternary alloys for oxygen electroreduction. *Phys. Chem. Chem. Phys.* **2008**, *10*, 3731−3738.
(25) Hwang, S. M.; Lee, C. H.; Kim, J. J.; Moffat, T. P. Oxygen Reduction Reaction on Electrodeposited $Pt_{100-x-y}Ni_xPd_y$ Thin Films. *Electrochim. Acta* **2010**, *55*, 8938−8946.
(26) Prochaska, M.; Jin, J.; Rochefort, D.; Zhuang, L.; DiSalvo, F. J.; Abruna, H. D.; van Dover, R. B. High Throughput Screening of Electrocatalysts for Fuel Cell Applications. *Rev. Sci. Instrum.* **2006**, 77.
(27) Stamenkovic, V. R.; Mun, B. S.; Mayrhofer, K. J. J.; Ross, P. N.; Markovic, N. M. Effect of Surface Composition on Electronic Structure, Stability, and Electrocatalytic Properties of Pt-Transition Metal Alloys: Pt-Skin versus Pt-Skeleton Surfaces. *J. Am. Chem. Soc.* **2006**, *128*, 8813−8819.
(28) Wang, C.; Chi, M. F.; Li, D. G.; Strmcnik, D.; van der Vliett, D.; Wang, G. F.; Komanicky, V.; Chang, K. C.; Paulikas, A. P.; Tripkovic, D.; et al. Design and Synthesis of Bimetallic Electrocatalyst with Multilayered Pt-Skin Surfaces. *J. Am. Chem. Soc.* **2011**, *133*, 14396−14403.
(29) van der Vliet, D.; Wang, C.; Li, D.; Paulikas, A. P.; Greeley, J.; Rankin, R. B.; Strmcnik, D.; Tripkovic, D.; Markovic, N. M.; Stamenkovic, V. R. Unique Electrochemical Adsorption Properties of Pt-Skin Surfaces. *Angew. Chem., Int. Ed.* **2012**, *51*, 3139−3142.
(30) Stamenkovic, V.; Mun, B. S.; Mayrhofer, K. J. J.; Ross, P. N.; Markovic, N. M.; Rossmeisl, J.; Greeley, J.; Nørskov, J. K. Changing the Activity of Electrocatalysts for Oxygen Reduction by Tuning the Surface Electronic Structure. *Angew. Chem., Int. Ed.* **2006**, *45*, 2897−2901.

(31) Greeley, J.; Stephens, I. E. L.; Bondarenko, A. S.; Johansson, T. P.; Hansen, H. A.; Jaramillo, T. F.; Rossmeisl, J.; Chorkendorff; Nørskov, J. K. Alloys of Platinum and Early Transition Metals As Oxygen Reduction Electrocatalysts. *Nat. Chem.* **2009**, *1*, 552−556.
(32) Stamenkovic, V.; Mun, B. S.; Mayrhofer, K. J. J.; Ross, P. N.; Markovic, N. M.; Rossmeisl, J.; Greeley, J.; Nørskov, J. K. Changing the Activity of Electrocatalysts for Oxygen Reduction by Tuning the Surface Electronic Structure. *Angew. Chem. Inter. Ed.* **2006**, *45*, 2897−2901.
(33) Greeley, J.; Nørskov, J. K. Combinatorial Density Functional Theory-Based Screening of Surface Alloys for the Oxygen Reduction Reaction. *J. Phys. Chem. C* **2009**, *113*, 4932−4939.
(34) Sun, S. H.; Murray, C. B.; Weller, D.; Folks, L.; Moser, A. Monodisperse FePt Nanoparticles and Ferromagnetic FePt Nanocrystal Superlattices. *Science* **2000**, *287*, 1989−1992.
(35) Wang, C.; Chi, M. F.; Li, D. G.; van der Vliet, D.; Wang, G. F.; Lin, Q. Y.; Mitchell, J. F.; More, K. L.; Markovic, N. M.; Stamenkovic, V. R. Synthesis of Homogeneous Pt-Bimetallic Nanoparticles as Highly Efficient Electrocatalysts. *ACS Catal.* **2011**, *1*, 1355−1359.
(36) Wang, C.; Markovic, N. M.; Vojislav, V. R. Advanced Platinum Alloy Electrocatalysts for the Oxygen Reduction Reaction. *ACS Catal.* **2012**, *2*, 891−898.
(37) Wang, C.; van der Vilet, D.; Chang, K. C.; You, H. D.; Strmcnik, D.; Schlueter, J. A.; Markovic, N. M.; Stamenkovic, V. R. Monodisperse Pt_3Co Nanoparticles as a Catalyst for the Oxygen Reduction Reaction: Size-Dependent Activity. *J. Phys. Chem. C* **2009**, *113*, 19365−19368.
(38) Wang, C.; Wang, G. F.; van der Vliet, D.; Chang, K. C.; Markovic, N. M.; Stamenkovic, V. R. Monodisperse Pt_3Co Nanoparticles As Electrocatalyst: The Effects of Particle Size and Pretreatment on Electrocatalytic Reduction of Oxygen. *Phys. Chem. Chem. Phys.* **2010**, *12*, 6933−6939.
(39) Li, D.; Wang, C.; Tripkovic, D.; Sun, S.; Markovic, N. M.; Stamenkovic, V. R. Surfactant Removal for Colloidal Nanoparticles from Solution Synthesis: The Effect on Catalytic Performance. *ACS Catal.* **2012**, *2*, 1358−1362.